Chemically-Resolved Volatility Measurements of Organic Aerosol from Different Sources

J. A. HUFFMAN,[†,‡] K. S. DOCHERTY,[†] C. MOHR,[†,§] M. J. CUBISON,[†] I. M. ULBRICH,[†,‡] P. J. ZIEMANN,[∥] T. B. ONASCH,[⊥] AND J. L. JIMENEZ*[,†,‡]

Cooperative Institute for Research in Environmental Sciences (CIRES), Boulder, Colorado; Department of Chemistry and Biochemistry, University of Colorado, Boulder, Colorado; Air Pollution Research Center, University of California—Riverside, Riverside, California; and Aerodyne Research, Inc., Billerica, Massachusetts

Received December 13, 2008. Revised manuscript received May 14, 2009. Accepted May 23, 2009.

A newly modified fast temperature-stepping thermodenuder (TD) was coupled to a High Resolution Time-of-Flight Aerosol Mass Spectrometer for rapid determination of chemically resolved volatility of organic aerosols (OA) emitted from individual sources. The TD-AMS system was used to characterize primary OA (POA) from biomass burning, trash burning surrogates (paper and plastic), and meat cooking as well as chamber-generated secondary OA (SOA) from α-pinene and gasoline vapor. Almost all atmospheric models represent POA as nonvolatile, with no allowance for evaporation upon heating or dilution, or condensation upon cooling. Our results indicate that all OAs observed show semivolatile behavior and that most POAs characterized here were at least as volatile as SOA measured in urban environments. Biomass-burning OA (BBOA) exhibited a wide range of volatilities, but more often showed volatility similar to urban OA. Paper-burning resembles some types of BBOA because of its relatively high volatility and intermediate atomic oxygen-to-carbon (O/C) ratio, while meat-cooking OAs (MCOA) have consistently lower volatility than ambient OA. Chamber-generated SOA under the relatively high concentrations used in traditional experiments was significantly more volatile than urban SOA, challenging extrapolation of traditional laboratory volatility measurements to the atmosphere. Most OAs sampled show increasing O/C ratio and decreasing H/C (hydrogen-to-carbon) ratio with temperature, further indicating that more oxygenated OA components are typically less volatile. Future experiments should systematically explore a wider range of mass concentrations to more fully characterize the volatility distributions of these OAs.

1. Introduction

Organic aerosol (OA) comprises an important fraction of the fine particle mass at most locations (*1*). The volatility of OA determines the likelihood that a compound will exist in the gas or particle phase, and thus strongly influences the concentration and lifetimes of OA through governing primary OA (POA) gas-particle partitioning and secondary OA (SOA) formation. Deposition rates of chemical species due to both wet and dry processes are greatly influenced by the phase of the species (*2*), and chemical mechanisms and rates of gas, liquid, and heterogeneous reactions of the same molecule can be very different. Many instruments can have sampling biases as a result of particle evaporation or condensation (*3*) and aircraft inlets are particularly susceptible to losses from heating (*4*). An accurate understanding of OA volatility is therefore important to properly predict the chemistry and phase-partitioning of both natural and anthropogenic OA species, and to properly interpret OA measurements.

POA, emitted into the atmosphere directly in the particle phase, has long been assumed to be nonvolatile in atmospheric models. Thus, the POA mass in models does not change when air masses are cooled, heated, or diluted, and POA is not considered a source of gas-phase species available for atmospheric oxidation and potential condensation as SOA. Recently, this assumption has been challenged (*5*−*7*), most notably by Robinson et al. (*5*), who suggested that evaporation of semivolatile POA is an important source of gas-phase material for SOA production. Meat-cooking emissions of POA (MCOA) can be a significant contributor to ambient OA by some estimates, accounting for as much fine POA mass as vehicles and up to 21% of the fine primary organic mass (*8*) in some locations. Biomass burning POA emitted from wild and agricultural fires and from wood-burning stoves (BBOA) can also be an important fraction of the total OA under many conditions. For example, biomass burning accounted for approximately 16% of the organic carbon in Mexico City during the MILAGRO 2006 campaign (*9*). POA from trash burning (TBOA) may be an important source in developing countries. The volatilities of these different types of POA are poorly constrained at present. SOA can comprise a large fraction of the ambient OA even in urban areas (*10*) and is significantly underestimated by current models in many environments (*11, 12*). While the semivolatility of SOA has been included in models for more than a decade, the relevant properties remain poorly constrained. Recently, Biswas et al. (*13*) showed that the production of reactive oxygen species, a surrogate for particle toxicity, is greatly reduced when the semivolatile fraction was removed from combustion exhaust particles, suggesting that this fraction may be more directly associated with human health effects.

Publications on aerosol volatility date back to at least the 1960s (*14*) and several groups have utilized heated tube ("thermodenuder") volatility measurements to infer particle composition by, for example, measuring changes in size distributions (e.g., ref *15*). Real-time chemically resolved measurements of OA volatility, however, have not been available until recently (*16*). This study applies this recently developed methodology to direct measurements of chemically resolved source volatility from BBOA, MCOA, TBOA, and chamber SOA.

2. Experimental Section

A recently developed thermodenuder (TD) (*16*) was placed upstream of a High-Resolution Time-of-Flight Aerosol Mass Spectrometer (AMS, Aerodyne Research) (*17, 18*) for several

* Corresponding author phone +1-303-492-3557; e-mail: jose.jimenez@colorado.edu.
[†] Cooperative Institute for Research in Environmental Sciences (CIRES).
[‡] Department of Chemistry and Biochemistry, University of Colorado.
[§] Now at Paul Scherrer Institute (PSI), Villigen, Switzerland.
[∥] Air Pollution Research Center, University of California-Riverside.
[⊥] Aerodyne Research, Inc.

10.1021/es803539d CCC: $40.75
Published on Web 06/12/2009

studies of aerosol sources. The TD consists of a 50-cm long, 2.5-cm OD stainless steel tube heated with a 3-zone temperature controller through which the sample air flows, leading to evaporation of some of the particle mass. A 50-cm charcoal diffusion denuder follows the heating section to adsorb vapors and prevent recondensation. A rapid-switching valve system toggles the AMS between sampling undenuded ambient air and TD-processed air every 1−10 min in order to acquire a rapidly interleaved data set. The TD-AMS system can measure from ambient temperature to ~230 °C in ~1 h. Detailed descriptions of both TD characterization and operation (*7, 16, 19*) and the effect of residence time on observed evaporation (*7, 20*) are available elsewhere. In each study described herein, air was sampled through a $PM_{2.5}$ cyclone and then through both the TD and a 1/4 inch bypass line at 0.6 lpm each. The TD was operated with the same set of instrumental settings (e.g., sample line configuration, flow rate, valve switching pattern) during all experiments to provide self-consistent data. All data shown here were corrected for experimentally determined particle number losses (*16*), due mostly to diffusion and thermophoresis, which increase with temperature from 5% at ambient to 20% at 230 °C. As a result, the decrease in MFR as a function of temperature is due primarily to particle mass evaporation. Comparisons of ammonium sulfate thermograms from laboratory and field experiments (*7*) showed similar results, giving confidence that the instrument behaves similarly in both environments. Changes in particle phase can in principle lead to collection efficiency (CE) changes as a function of temperature, although this issue appears to be small for ambient particles other than ammonium sulfate as discussed in previous publications (*7, 16*). It is also possible that particle size changes have an effect on the reported thermograms if significant mass enters or leaves the AMS size transmission window after evaporation (*7*), however this effect is estimated to be small for the experiments reported here based on the measured size distributions.

The TD-AMS was utilized during three aerosol source measurement campaigns. First, volatility of BBOA was measured during FLAME-1 (Fire Lab At Missoula Experiment, phase 1), which took place June 2006 at the US Forest Service Fire Sciences Lab (FSL) in Missoula, MT. The study analyzed highly diluted (~× 10^4) smoke from burns of ~18 different biomass specimens over one week, attempting to simulate wildfires. The smoke was confined to a large chamber and OA from flaming and smoldering phases of combustion of each biomass were allowed to mix and stabilize before starting the TD-AMS cycle. FLAME-1 and the FSL chamber are described in detail elsewhere (e.g. *21*).

Second, measurements of OA from meat-cooking and trash-burning emission sources were performed in a 240-m^3 aluminum shed located outside of Boulder, CO (*22*). All instruments were located inside the shed and sampled from an inlet placed near the top of the enclosed space. Emissions were sampled at dilution factors of ~100−1000, but at concentrations that were at least 10× the low rural background levels (~1 $\mu g\ m^{-3}$ OA). Meats were cooked on a propane grill under conditions similar to home-cooking procedures, and the air in the shed was purged between experiments by opening the door and using exhaust fans to exchange the air until the concentrations returned to background levels. A number of meats were cooked individually (*22*), of which four with the highest fat content and emissions are shown here because they are expected to be more important contributors in the real world, and because their signals were sufficiently high to provide good signal-to-noise and stay higher than ten times the ambient background OA during the TD cycle. Additionally, several types of plastic and paper were burned as examples of components of trash-burning. POA generated by burning plastic No. 2 (high-density polyethylene) and brown paper supermarket-style bags are shown.

Finally, SOA was generated from two well-studied VOC oxidation reactions in an environmental chamber (*23*) located in the Ziemann laboratory at UC−Riverside. In the first reaction α-pinene reacted with O_3, and in the second gasoline vapor was photooxidized in the presence of NO_x (producing SOA that should be dominated by reaction products from aromatic precursors (*24*)). These reactions produced typical biogenic and anthropogenic SOA and had total aerosol concentrations of 500 and 60 $\mu g/m^3$, respectively. Recent studies have shown that SOA formed with lower concentrations is less volatile (e.g., ref *25*), however, the conditions used here are typical of those used for most SOA model development until recently (e.g., ref *24*). Characterization of this SOA is therefore still of interest, since these models are widely used at present and will likely continue to be used for years.

The relationship of the relative volatility determined with a TD and the mass concentration in the experiment has been studied by Faulhaber et al. (*19*), who observed 5−10 °C shifts in the thermograms of pure-component particles after changing mass concentration over a large range (~0−600 $\mu g/m^3$). TD thermograms are partially a measure of relative volatility, and since a larger OA concentration also carries with it a larger concentration of semivolatile VOCs (SVOCs), the ways in which thermograms change as mass concentration is reduced can become complex. This effect is experimentally characterized below and found to be smaller than the differences caused by chemical composition in the few cases for which data is available. We also note that the volatility of POA at concentrations higher than ambient is of direct interest since (a) POA emission factors have often been determined at elevated concentrations similar to those used here, and such factors may be too high when dilution to ambient levels occurs with volatility being the key property that determines the reduction in emission factor; and (b) during the equilibration to ambient levels, the evaporated material is a source of SVOCs with saturation conditions that are only 1−2 orders of magnitude above ambient OA levels, and which should be very efficient SOA precursors (*5*).

3. Results and Discussion

3.1. Biomass-Burning Organic Aerosol Volatility. Primary BBOA emissions were measured as part of FLAME-1, and thermograms (mass fraction remaining, MFR, vs calibrated centerline TD temperature) of total OA mass for two examples are shown in Figure 1a. These two biomasses (dried lodgepole pine needles and sticks, and a mix of Utah sage and rabbitbrush sticks and foliage) bracket the range of behaviors that have been measured by the TD-AMS system for any OA, with evaporation rates within the TD of 1.6 and 0.2% K^{-1} near ambient temperature, respectively (measured between ambient and 50 °C). Figure 1b shows the same biomasses, but using the high resolution marker $C_2H_4O_2^+$ (m/z 60) for levoglucosan and similar species such as galactosan and mannosan (*21*) (totaling ~3 × levoglucosan in Mexico City (*26*), which is often used as an AMS tracer for biomass burning. Because the shapes of most thermograms are smooth, we use the temperature at which 50% of the mass has evaporated (T_{50}) as a concise metric for comparing experiments. Vapor pressure distributions or lumped surrogate enthalpies of vaporization can be estimated from these results with additional assumptions, which however introduce several complications (*19, 27, 28*). In this first work, we focus on a qualitative survey of volatility trends with comparisons to those for ambient OA in Mexico City (*7*). The TD-AMS was also deployed to Riverside, CA with results very similar to those in Mexico City (*7*). We will explore the quantitative interpretation of the results herein in future work.

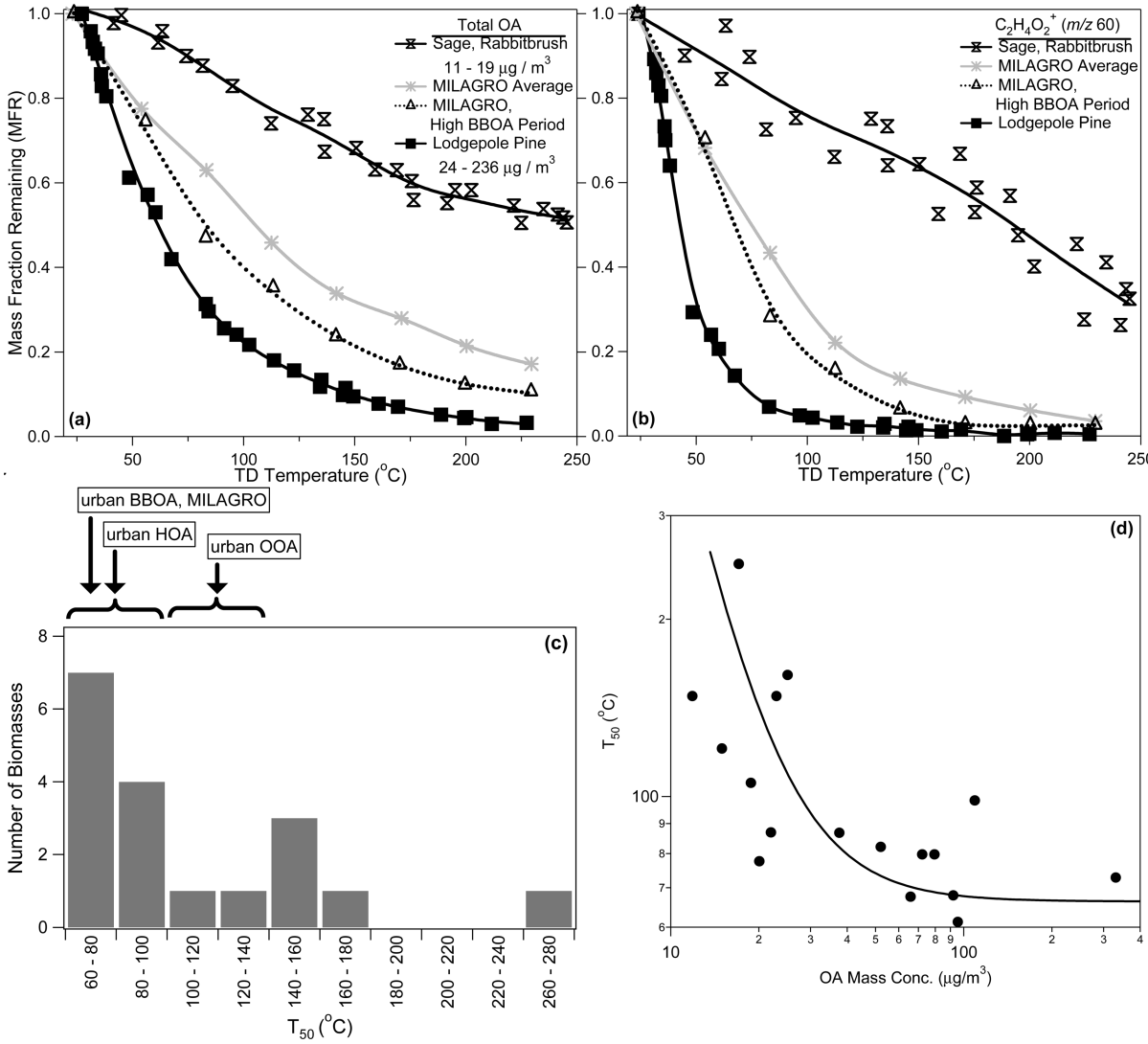

FIGURE 1. (a) Total primary BBOA thermograms showing median mass fraction remaining (MFR) vs TD temperature for BBOA from the FLAME-1 experiments. Spline fits are shown as guides to the eye. Also shown are the average thermograms for total OA in Mexico City during MILAGRO, and the thermogram of ambient OA during a 3-h morning period in that campaign when BBOA was the dominant OA type due to heavy impact from a forest fire plume. (b) Thermograms of BBOA marker ion $C_2H_4O_2^+$ (*m*/*z* 60) for same samples as in Part (a). The $C_2H_4O_2^+$ signal was 6% the total OA signal for the Lodgepole Pine BBOA and 1% for Sage/Rabbitbrush BBOA. (c) Histogram of T_{50} values for 18 different BBOAs measured during FLAME-1. (d) Log−log plot of OA volatility (T_{50}) vs average OA mass concentration for each burn. Spline curve is added as a guide to the eye.

Figure 1c summarizes results for the 18 different BBOAs in a histogram of T_{50} values. While BBOA produced by burning lodgepole pine (T_{50} = 61 °C) exhibits the lowest MFR as a function of temperature for all OAs analyzed, many BBOAs from FLAME-1 also show relatively high volatility (T_{50} < 100 °C). Conversely, BBOA produced by burning sage and rabbitbrush (T_{50} = 248 °C) shows the highest MFR of any OA measured to date with the TD-AMS. A large variability in BBOA volatility has also been observed in ambient air, with MILAGRO BBOA being close to the high volatility end (Figure 1a and ref *7*). Grieshop et al. (*29*) also recently reported the relatively high volatility of woodstove BBOA emissions, which had T_{50} values of ~42 °C in a TD setup similar to ours. They also showed that unit resolution *m*/*z* 60 was one of the more volatile components in the MS from both fresh and aged wood-burning emissions. Aircraft measurements during ICARTT reported a BBOA with much lower volatility (MFR ~25% at 400 °C (*30*)), though the much shorter RT (~1s) used for this study would lead to higher MFR and complicates direct comparison.

The more volatile BBOAs were generally dominated by smoldering combustion, while the less volatile ones were more influenced by flaming combustion (characterized by both visual inspection and modified combustion efficiency). T_{50} values are plotted versus the average OA concentration in Figure 1d to illustrate the correlation of high OA-emitting smoldering-dominated burns with relatively high volatility BBOA, and less OA-emitting flaming-dominated burns with lower volatility BBOA. Note that the higher concentrations enhance gas-to-particle partitioning, thus accentuating the observed trend. However, the main cause for the observed volatility differences are the differences in chemical composition, as repeat measurements at some temperatures at different concentration levels show small differences in MFR, and the large differences in MFR are apparent for different biomasses when sampling similar concentrations (Figure S1−S3 of the Supporting Information). The volatility of most observed BBOA under the conditions of FLAME-1 is similar to or higher than that of urban OA, although much less volatile BBOAs are possible.

Oja and Suuberg (*31*) report the vapor pressure of levoglucosan at 68 °C as 1×10^{-4} mbar, which corresponds to a saturation concentration of 600 μg m^{-3}, indicating that levoglucosan should appear as relatively volatile within the

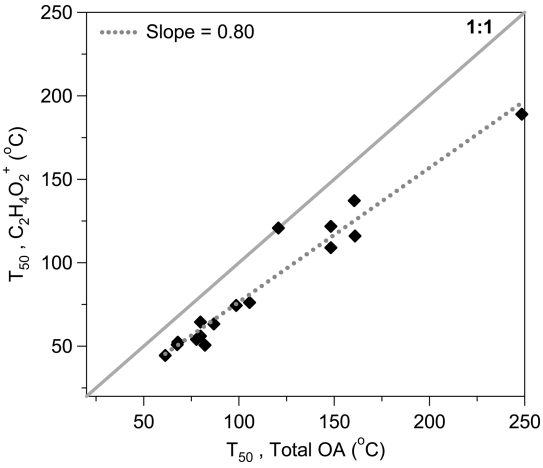

FIGURE 2. Relationship of T_{50} for the $C_2H_4O_2^+$ BBOA marker ion (m/z 60) and total BBOA for 18 different primary BBOAs measured during FLAME-1.

TD-AMS. As expected, therefore, the marker for levoglucosan-like species ($C_2H_4O_2^+$) is consistently more volatile than the total OA, but the T_{50} for each are highly correlated for individual sources (Figure 2). The composition of the species that give rise to this marker signal at m/z 60 does not change greatly between biomasses (*21*), thus it is likely that the differences in T_{50} of m/z 60 for different biomasses are due to reduced evaporation of the same levoglucosan-like species when embedded in a less-volatile matrix. The high correlation also suggests that the $C_2H_4O_2^+$ ion can be used as a marker in ambient measurements to estimate the total BBOA volatility when the signal at this ion is dominated by BBOA.

Atomic oxygen- and hydrogen-to-carbon (O/C, H/C) ratios were estimated directly from the high-resolution mass spectra using the technique developed by Aiken et al. (*32, 33*). The evolution of these ratios with TD temperature after partial evaporation of the two BBOAs discussed here are shown in Figure 3a,b. Both O/C curves show an average increase from ambient temperature to the hottest set-point, although the curve for the lodgepole pine dips between ambient temperatures and ~65 °C. H/C decreases with temperature in both cases. This indicates that the most oxidized species in each BBOA are less volatile than the more reduced species. With increasing TD temperature the more volatile species evaporate, leaving less volatile, more oxidized species in the particles. The overall lower volatility of the sage and rabbitbrush BBOA is consistent with its higher O/C ratio. The increase in O/C and decrease in H/C with temperature for both BBOAs is similar to ambient observations made during two megacity studies, which showed that POA (from BBOA and urban sources) was of similar or higher volatility to SOA, and that the most oxygenated OA (aged SOA) was the least volatile (*7*). While additional factors (i.e., molecular weight) affect the volatility of a given OA mixture, our results show the degree of oxidation (i.e., O/C) is an important factor in determining aerosol volatility. We note that we cannot rule out the possibility that chemical reactions induced by

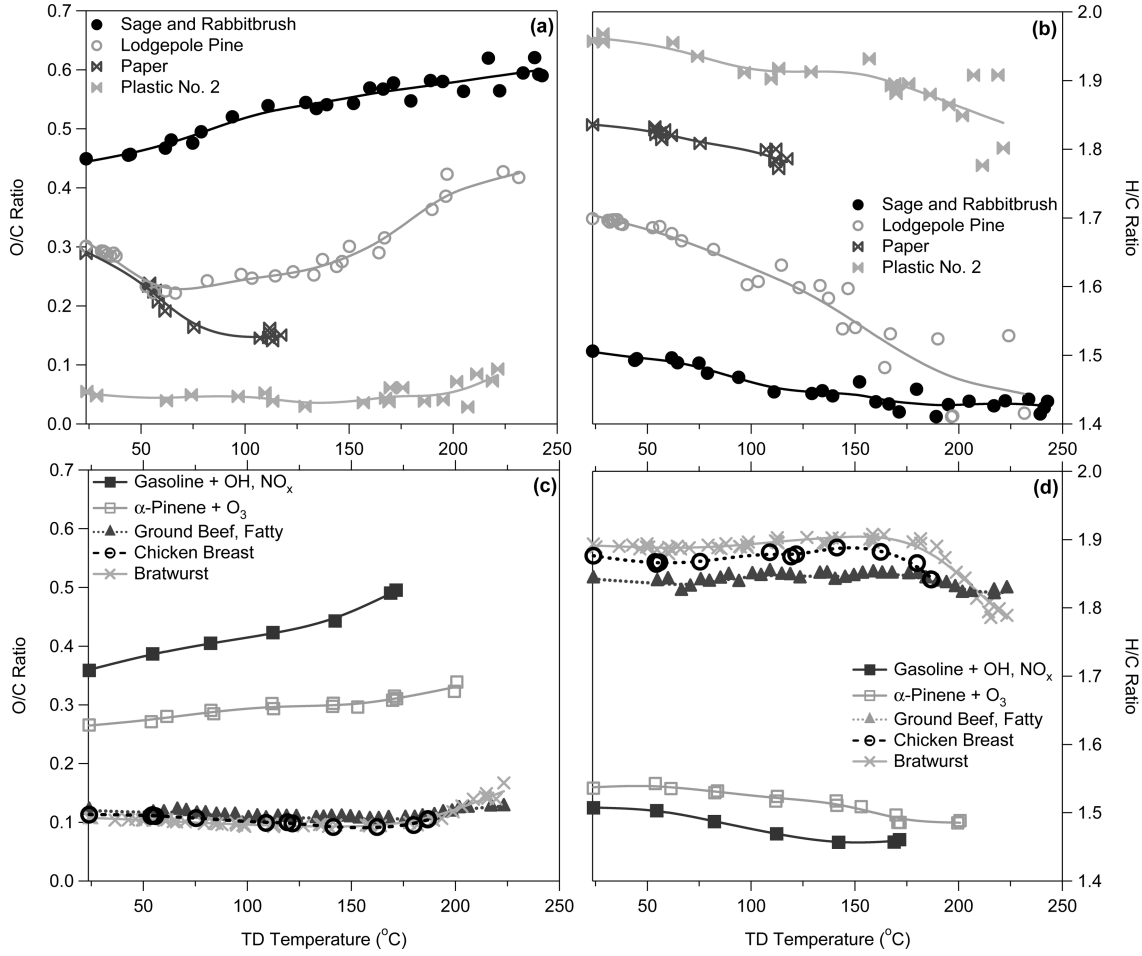

FIGURE 3. Elemental composition of the OAs studied here as a function of TD temperature. Left panels show oxygen-to-carbon (O/C) ratios and right panels show hydrogen-to-carbon (H/C) ratios. (a,b) Primary BBOAs and TBOAs; (c,d) chamber SOAs and primary MCOAs. The absolute accuracies of the O/C and H/C estimates are estimated at 31% and 10%, respectively, while the relative precision is ± 3% in each case (*33*).

TD heating, especially at the highest temperatures, could alter the particle composition, and thereby affect the observed trends.

3.2. Meat-Cooking and Trash-Burning OA Volatility. As described by Mohr et al. (*22*), the MCOA mass spectra are hydrocarbon-like and dominated by reduced ions (C_xH_y). $C_3H_7^+$ (*m*/*z* 43) and $C_4H_7^+$ (*m*/*z* 55) are consistently the most abundant ions in the MS, while the relative contribution from oxygenated ions is considerably lower. The O/C ratios of ∼0.11−0.14 are similar to those of typical fatty acids (e.g. oleic acids) and much lower than for ambient urban OOA. The $C_3H_3O^+$ ion (*m*/z 55) was the most abundant oxygenated ion present in each of the MCOAs shown here, with 40−50% of the signal of the highest reduced ion peak. The MS of plastic TBOA were similar to those of MCOA, with even lower relative abundance of oxygenated ions and lower O/C than the meats (0.08) (*22*). In contrast to the MCOA, however, in the MS of TBOA produced by burning plastic No. 2 (high-density polyethylene, HDPE) $C_2H_3O^+$ (*m*/z 43) was the most abundant oxygenated peak, with approximately 16% of the intensity of the $C_3H_7^+$ peak. Results from plastic No. 4 (low-density polyethylene, LDPE) are almost identical (not shown). Paper burning emissions were markedly different from these, with an MS similar to BBOA produced from pine burning in FLAME-1 in which both reduced and oxygenated ions make significant contributions, the O/C (0.31) is an intermediate value, and $C_2H_4O_2^+$ (*m*/z 60) was a dominant peak in the spectrum. None of the sources sampled here had significant emissions of nonrefractory inorganic aerosol.

Figure 4a−d shows thermograms of total OA from each source as well as of major individual high-resolution (HR) ions, and compare them to the average urban aerosol in Mexico City during MILAGRO (*7, 16*). The three MCOAs show complex volatility behavior, with MFRs initially similar to urban OA (bratwurst MCOA evaporates at rate of 0.7%K^{-1} near ambient *T*) but then lower as the TD temperature was increased. This suggests a bimodal volatility distribution with the majority of the mass having low volatility. This is not unexpected, since composition of MCOA particles are thought to be dominated by low-volatility fatty acids that evaporate at high cooking temperatures and then condense (*22, 34*).

Consistent with the ambient urban OA observations (*7*), the differences in volatility between $C_xH_y^+$ ions are smaller than for $C_xH_yO_z^+$ ions. The $C_4H_7^+$ ion is shown in each of the MCOA thermograms to represent the reduced ions, because it is the most abundant ion in each of the MCOA spectra and its thermogram has a similar profile to that of the total MCOA. Most of the important $C_xH_y^+$ and $C_xH_yO_z^+$ ions have similar thermograms and slopes as $C_4H_7^+$, with positive or negative offsets. The $C_2H_4O_2^+$ ion is also shown in MCOA thermograms, where both it and $C_3H_5O_2^+$ (not shown) exhibit unique profiles when compared to those of other $C_xH_yO_z^+$ ions. This difference indicates that these ions arise from a different set of compounds in the MCOA. The dependence of MCOA O/C and H/C ratios on TD temperature are shown in Figure 3c,d, and are very similar to each other, consistent with the high similarity in their mass spectra (*22*). This suggests that the major components of MCOA produced by cooking different meats are similar. The atomic ratios of MCOAs also show little change with increasing temperature, except at the hottest values (>175 °C), where again there is an increase in O/C and a decrease in H/C.

TBOA produced by burning paper is considerably more volatile than the average ambient urban OA, consistent with the similarity of its MS to that of pine-burning OA from FLAME-1 (*22*). TBOA from plastic shows approximately the same volatility (0.8% K^{-1} near ambient *T*) as average urban OA, but with a smaller residual mass fraction at the highest temperatures. The thermograms of the reduced ions in TBOA MS (Figure 4d) again show a narrow spread, whereas those of the oxygenated ions are more varied. The $C_2H_4O_2^+$ ion in the MS from paper-burning OA (*m*/*z* 60, and similarly $C_3H_5O_2^+$, *m*/*z*73, also a BBOA tracer ion, not shown) decreases faster with increasing temperature than the total OA, consistent with the observations from BBOA (Figure 2). The paper burning experiment was unique because the thermograms of the oxygenated ions (excluding CO_2^+), although more variable with respect to one another than the $C_xH_y^+$ ions also showed consistently higher volatility than the $C_xH_y^+$ ions. The H/C ratios for both TBOAs shows a slight decrease with temperature, while the O/C ratio of plastic TBOA behaves similar to those of the MCOAs, being nearly constant with a small increase at the highest temperatures (Figure 3a,b). The O/C ratio of the paper-burning TBOA initially decreases, again similar to the behavior of the pine BBOA. Unfortunately, data at higher temperatures are not available.

3.3. Volatility of Chamber SOA. Figure 4e shows the thermograms of SOA formed from both chamber reactions, which appear to be significantly more volatile than the average OA from MILAGRO and the ambient oxygenated OA (OOA, an SOA surrogate: refs *1,10,12,18,22,33* and *35*) from Mexico City and Riverside, CA (*7*). Both types of SOA had T_{50} values of 84 °C or less, similar to ambient urban OA during periods strongly influenced by urban POA, but much lower than the 106 °C value measured for the average urban total OA and 110−130 °C for urban SOA (*7*). This indicates, therefore, that SOA formed from these two chamber reactions under conditions typical of those used to develop traditional SOA models (*24*) is more volatile than the SOA measured in polluted urban environments. Part of this difference may be due to higher OA concentrations in the chamber, as discussed above. However, ambient submicrometer OA concentration in Mexico City was ∼1/3 of that present during our gasoline photooxidation experiment. It is thus unlikely that this effect can explain the magnitude of the differences observed. Rather, additional aging or the influence of other precursors and particle-phase reactions (e.g., ref *35*) may be responsible for the lower volatility of ambient SOA. Stanier et al. (*28*) have recently studied the effects of temperature on SOA formed from α-pinene ozonolysis, observing evaporation of 0.4 to 3.6% K^{-1} near ambient temperature, which encompasses the value of 1% K^{-1} reported here. Our observed evaporation of 0.9% K^{-1} near ambient temperatures for SOA formed from the photooxidation of gasoline vapor is lower than the 1.9 to 2.4% K^{-1} range of values calculated for toluene SOA from observations by Offenberg et al. (*27*). However, the difference may be partially due to the longer residence time used in that study, which was about twice that of our study.

Figure 4f shows that the species associated with the CO_2^+ ion in the chamber-generated SOA were considerably more volatile than in the MILAGRO study, consistent with trends in total OA. This again supports the conclusion that ambient urban SOA is significantly less volatile than SOA generated under conditions of many traditional experiments. Using SOA yields and vapor pressures obtained from fits to these chamber data in atmospheric models will thus likely overestimate ambient SOA volatility, as will the use of volatilities obtained from direct measurements on chamber-generated SOA under high concentrations.

Figure 3c,d shows the estimated average O/C and H/C ratios as a function of temperature for the two chamber-generated SOAs. Both show a slight increase in O/C and decrease in H/C with increasing temperature, with the SOA formed from gasoline photooxidation SOA being about

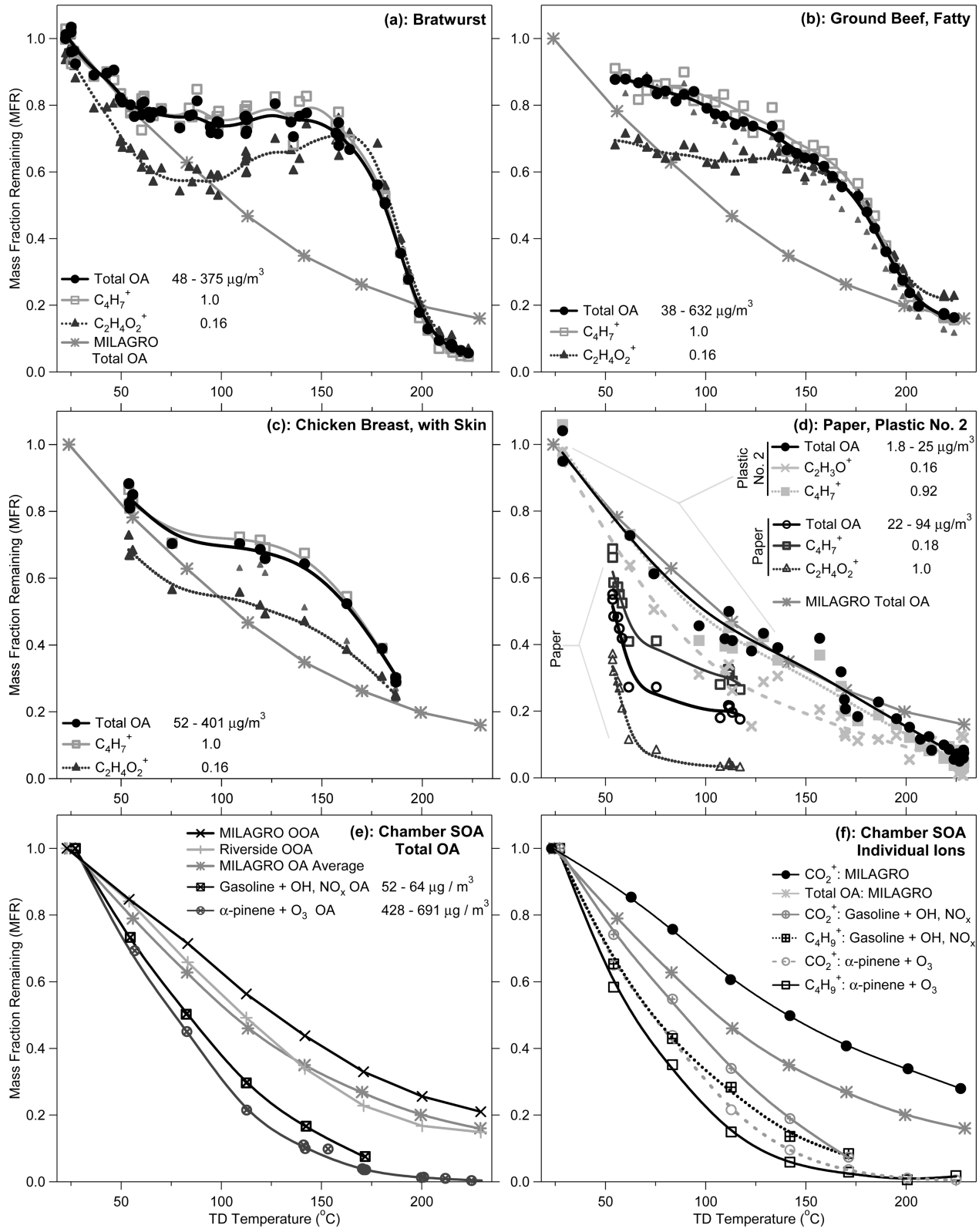

FIGURE 4. Thermograms of total OA and individual high-resolution ions from meat-cooking and trash-burning POA and chamber SOA experiments. Total OA from MILAGRO is also plotted on each graph for visual comparison. (a) bratwurst (b) ground beef, fatty, (c) chicken breast with skin, (d) paper and plastic burning, (e) total OAs of two chamber-generated SOA reactions compared to ambient urban OA and total ambient OOA (SOA), separated from total OA by positive matrix factorization (PMF) analysis (f) individual ions for more-oxygenated and more-reduced species for chamber-generated SOA, compared to urban OA and CO_2^+. The MFR of $C_2H_4O_2^+$ (a) increases from ~75−160 °C, possibly due to chemistry or matrix effects in the TD, or changes in AMS collection efficiency.

0.1 higher in O/C and lower in H/C compared to that formed from α-pinene ozonolysis. The O/C ratios of chamber-generated SOA at ambient temperature are lower than those of ambient OOA/SOA (0.5−1 (*33*)), which is consistent with the higher volatility of chamber-generated SOA, given the inverse correlation between oxygenation and volatility observed for most ambient OA and OA sources.

Acknowledgments

The authors would also like to thank J. Kimmel, E. Dunlea, M. Northway, D. Salcedo, and A. Trimborn for assistance in collecting data and J. Jayne and D. Worsnop for useful discussions. We also thank the organizers of FLAME-1 (S. Kreidenweis, C. Wold, W. Hao, and W. Malm) and the Niwot Source Emissions Study (M. Hannigan and M. Lechner). These studies were partially supported by Grant Nos. EPA STAR R831080, RD-83216101-0, and R833747, DOE (BER, ASP Program) DE-FG02-05ER63981, NSF ATM-0449815, and ATM-0528634, by NASA fellowships NGT5-30516 and NNG05GQ50H. Neither agency has reviewed these results and thus no endorsement should be inferred.

Supporting Information Available

This material is available free of charge via the Internet at http://pubs.acs.org.

Literature Cited

(1) Zhang, Q.; et al. Ubiquity and dominance of oxygenated species in organic aerosols in anthropogenically-influenced northern hemisphere mid-latitudes. *Geophys. Res. Lett.* **2007**, *34*, L13801.
(2) Bidleman, T. F. Atmospheric Processes. *Environ. Sci. Technol.* **1988**, *22*, 361–367.
(3) Biswas, P.; et al. Distortion of size distributions by condensation and evaporation in aerosol instruments. *Aerosol Sci. Technol.* **1987**, *7*, 231–246.
(4) Wilson, J. C.; Seebaugh, W. R., Chapter 30: Measurement of Aerosol from Aircraft. In *Aerosol Measurement: Principles, Techniques, and Applications, 2nd ed.*; Baron, P. A.; Willeke, K., Eds. Wiley-Interscience: New York, 2001; p894.
(5) Robinson, A. L.; et al. Rethinking organic aerosols: Semivolatile emissions and photochemical aging. *Science* **2007**, *315*, 1259–1262.
(6) Lipsky, E. M.; Robinson, A. L. Effects of dilution on fine particle mass and partitioning of semivolatile organics in diesel exhaust and wood smoke. *Environ. Sci. Technol.* **2006**, *40*, 155–162.
(7) Huffman, J. A.; et al. Chemically-resolved aerosol volatility measurements from two megacity field studies. *Atmos. Chem. Phys. Discuss.* **2009**, *9*, 2645–2697.
(8) Hildemann, L. M.; et al. Chemical Composition of Emissions from Urban Sources of Fine Organic Aerosol. *Environ. Sci. Technol.* **1991**, *25*, 744–759.
(9) Stone, E. A.; et al. Source apportionment of fine organic aerosol in Mexico City during the MILAGRO experiment 2006. *Atmos. Chem. Phys.* **2008**, *8*, 1249–1259.
(10) Docherty, K. S.; et al. Apportionment of primary and secondary organic aerosols in southern California during the 2005 study of organic aerosols in riverside (SOAR). *Environ. Sci. Technol.* **2008**, *42*, 7655–7662.
(11) Heald, C. L., et al. A large organic aerosol source in the free troposphere missing from current models. *Geophys. Res. Lett.* 2005, *32*, L18809.
(12) Volkamer, R., et al. Secondary organic aerosol formation from anthropogenic air pollution: Rapid and higher than expected. *Geophys. Res. Lett.* 2006, *33*, L17811.
(13) Biswas, S.; et al. Oxidative potential of semi-volatile and non volatile particulate matter (PM) from heavy-duty vehicles retrofitted with emission control technologies. *Environ. Sci. Technol.* **2009**, *43*, 3905–3912.
(14) Goetz, A.; et al. The metastability of natural and urban aerosols. *Pure Appl. Geophys.* **1961**, *50*, 67–80.
(15) Moore, K. G., et al. Long-range transport of continental plumes over the Pacific Basin: Aerosol physiochemistry and optical properties during PEM-Tropics A and B. *J. Geophys. Res.-Atmos.* 2003, *108*, D28236.
(16) Huffman, J. A.; et al. Development and characterization of a fast-stepping/scanning thermodenuder for chemically-resolved aerosol volatility measurements. *Aerosol Sci. Technol.* **2008**, *42*, 395–407.
(17) DeCarlo, P. F.; et al. Field-deployable, high-resolution, time-of-flight aerosol mass spectrometer. *Anal. Chem.* **2006**, *78*, 8281–8289.
(18) Canagaratna, M. R.; et al. Chemical and microphysical characterization of ambient aerosols with the aerodyne aerosol mass spectrometer. *Mass Spectrom. Rev.* **2007**, *26*, 185–222.
(19) Faulhaber, A.; et al. Characterization of a thermodenuder-particle beam mass spectrometer system for the study of organic aerosol volatility and composition. *Atmos. Meas. Tech.* **2009**, *2*, 15–31.
(20) An, W. J.; et al. Aerosol volatility measurement using an improved thermodenuder: Application to secondary organic aerosol. *J. Aerosol Sci.* **2007**, *38*, 305–314.
(21) Sullivan, A. P., et al. A Method for smoke marker measurements and its potential application for determining the contribution of biomass burning from wildfires and prescribed fires to ambient PM2.5 organic carbon. *J. Geophys. Res.* 2008, *113*, D22302.
(22) Mohr, C.; et al. Characterization of primary organic aerosol emissions from meat cooking, trash burning, and mobile sources with high-resolution aerosol mass spectrometry and comparison with ambient and chamber observations. *Environ. Sci. Technol.* **2009**, *43*, 2443–2449.
(23) Prenni, A. J., et al. Cloud droplet activation of secondary organic aerosol. J. Geophys. Res.-Atmos. 2007, *112*, D10223.
(24) Odum, J. R.; et al. Aromatics, reformulated gasoline, and atmospheric organic aerosol formation. *Environ. Sci. Technol.* **1997**, *31*, 1890–1897.
(25) Shilling, J. E.; et al. Loading-dependent elemental composition of α-pinene SOA particles. *Atmos. Chem. Phys. Discuss.* **2008**, *8*, 15343–15373.
(26) Aiken, A. C.; et al. Mexico City aerosol analysis during MILAGRO using high resolution aerosol mass spectrometry at the urban supersite (T0) - Part 1: Fine particle composition and organic source apportionment. *Atmos. Chem. Phys. Discuss.* **2009**, *9*, 8377–8427.
(27) Offenberg, J. H.; et al. Thermal properties of secondary organic aerosols. *Geophys. Res. Lett.* **2006**, *33*, L03816.
(28) Stanier, C. O.; et al. Measurements of the volatility of aerosols from α-pinene ozonolysis. *Environ. Sci. Technol.* **2007**, *41*, 2756–2763.
(29) Grieshop, A. P.; et al. Laboratory investigation of photochemical oxidation of organic aerosol from wood fies 1: measurement and simulation of organic aerosol evolution. *Atmos. Chem. Phys.* **2009**, *9*, 1263–1277.
(30) Clarke, A., et al. Biomass burning and pollution aerosol over North America: Organic components and their influence on spectral optical properties and humidification response. *J. Geophys. Res.* 2007, *112*, D12S18.
(31) Oja, V.; Suuberg, E. M. Vapor pressures and enthalpies of sublimation of D-glucose, D-xylose, cellobiose, and levoglucosan. *J. Chem. Eng. Data* **1999**, *44*, 26–29.
(32) Aiken, A. C.; et al. Elemental analysis of organic species with electron ionization high-resolution mass spectrometry. *Anal. Chem.* **2007**, *79*, 8350–8358.
(33) Aiken, A. C.; et al. O/C and OM/OC ratios of primary, secondary, and ambient organic aerosols with a high resolution time-of-flight aerosol mass spectrometer. *Environ. Sci. Technol.* **2008**, *42*, 4478–4485.
(34) Rogge, W. F.; et al. Sources of fine organic aerosol: 1. Charbroilers and meat cooking operations. *Environ. Sci. Technol.* **1991**, *25*, 1112–1125.
(35) Volkamer, R., et al. A missing sink for gas-phase glyoxal in Mexico City: Formation of secondary organic aerosol. *Geophys. Res. Lett.* 2007, *34*, L19807.

ES803539D

Supplementary Information for

Chemically-Resolved Volatility Measurements of Organic Aerosol from Different Sources

J.A. Huffman, K.S. Docherty, C. Mohr, M.J. Cubison, I.M. Ulbrich, P.J. Ziemann, T.B. Onasch, and J.L. Jimenez

All Supplementary figures colored by total OA concentration in undenuded state.

Figure Captions:

Figure S1: Total primary BBOA thermograms showing median mass fraction remaining (MFR) vs. TD temperature for BBOA from the FLAME-1 experiments. Spline fits are shown as guides to the eye. Also shown are the average thermograms for total OA in Mexico City during MILAGRO, and the thermogram of ambient OA during a 3-hour morning period in that campaign when BBOA was the dominant OA type due to heavy impact from a forest fire plume.

Figure S2: Total primary BBOA thermograms for emissions from burning additional wood types. **(a)** Ponderosa pine (duff), **(b)** Alaskan core tundra (duff), **(c)** Southern California manzanita, **(d)** Utah juniper (foliage and sticks). The plots are colored by undenuded mass concentration. In all cases some temperatures are studied at different concentrations, and modest differences in evaporation are observed.

Figure S3: Thermograms of total OA and individual high-resolution ions from meat-cooking and trash-burning POA and chamber SOA experiments, colored by the undenuded mass concentration. Total OA from MILAGRO is also plotted on each graph for visual comparison. **(a)** bratwurst, **(b)** paper and plastic burning, **(c)** chicken breast with skin, **(d)** total OAs of two chamber-generated SOA reactions compared to ambient urban OA and total ambient OOA (SOA), separated from total OA by positive matrix factorization (PMF) analysis. Some temperatures are studied at different concentrations, and modest differences in evaporation are observed.

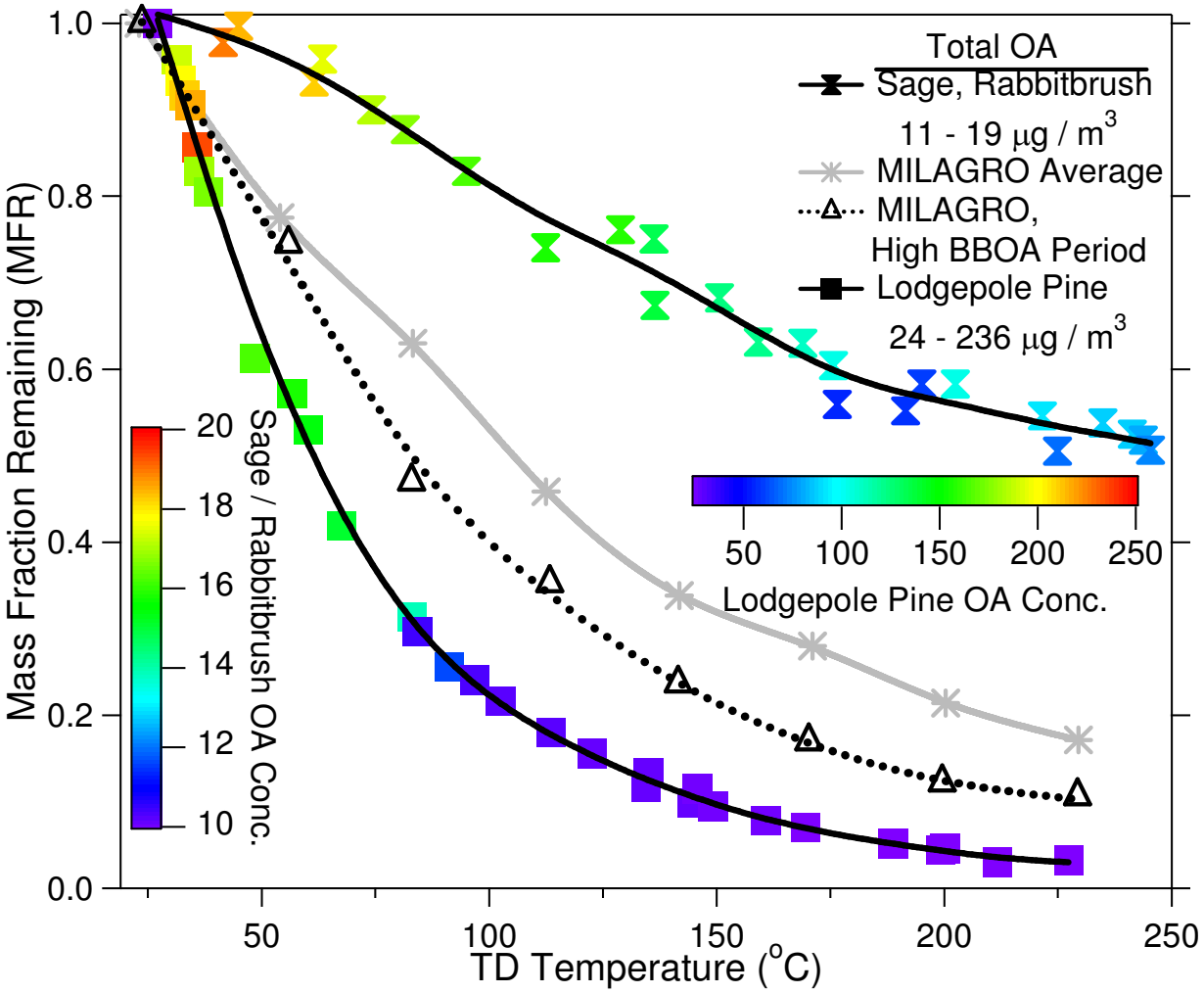
Mass Fraction Remaining (MFR)
1.0
0.8
0.6
0.4
0.2
0.0
50
100
150
200
250
TD Temperature (°C)
Total OA
Sage, Rabbitbrush
11 - 19 μg / m3
MILAGRO Average
MILAGRO,
High BBOA Period
Lodgepole Pine
24 - 236 μg / m3
50
100
150
200
250
Lodgepole Pine OA Conc.
Sage / Rabbitbrush OA Conc.
20
18
16
14
12
10

36 **Figure S1**

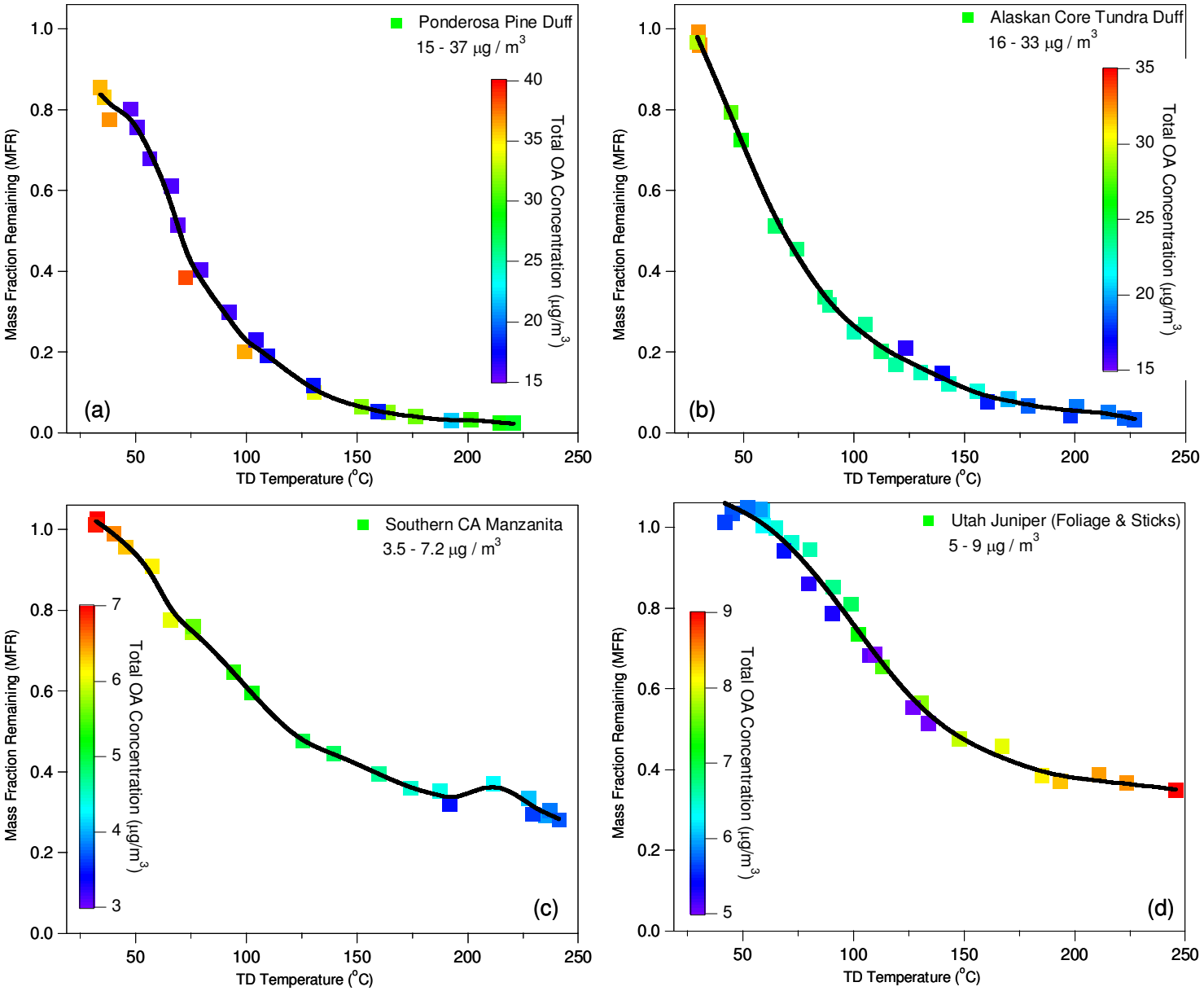
Ponderosa Pine Duff
15 - 37 µg / m3
(a)
Alaskan Core Tundra Duff
16 - 33 µg / m3
(b)
Southern CA Manzanita
3.5 - 7.2 µg / m3
(c)
Utah Juniper (Foliage & Sticks)
5 - 9 µg / m3
(d)
Mass Fraction Remaining (MFR)
TD Temperature (°C)
Total OA Concentration (µg/m3)

Figure S2

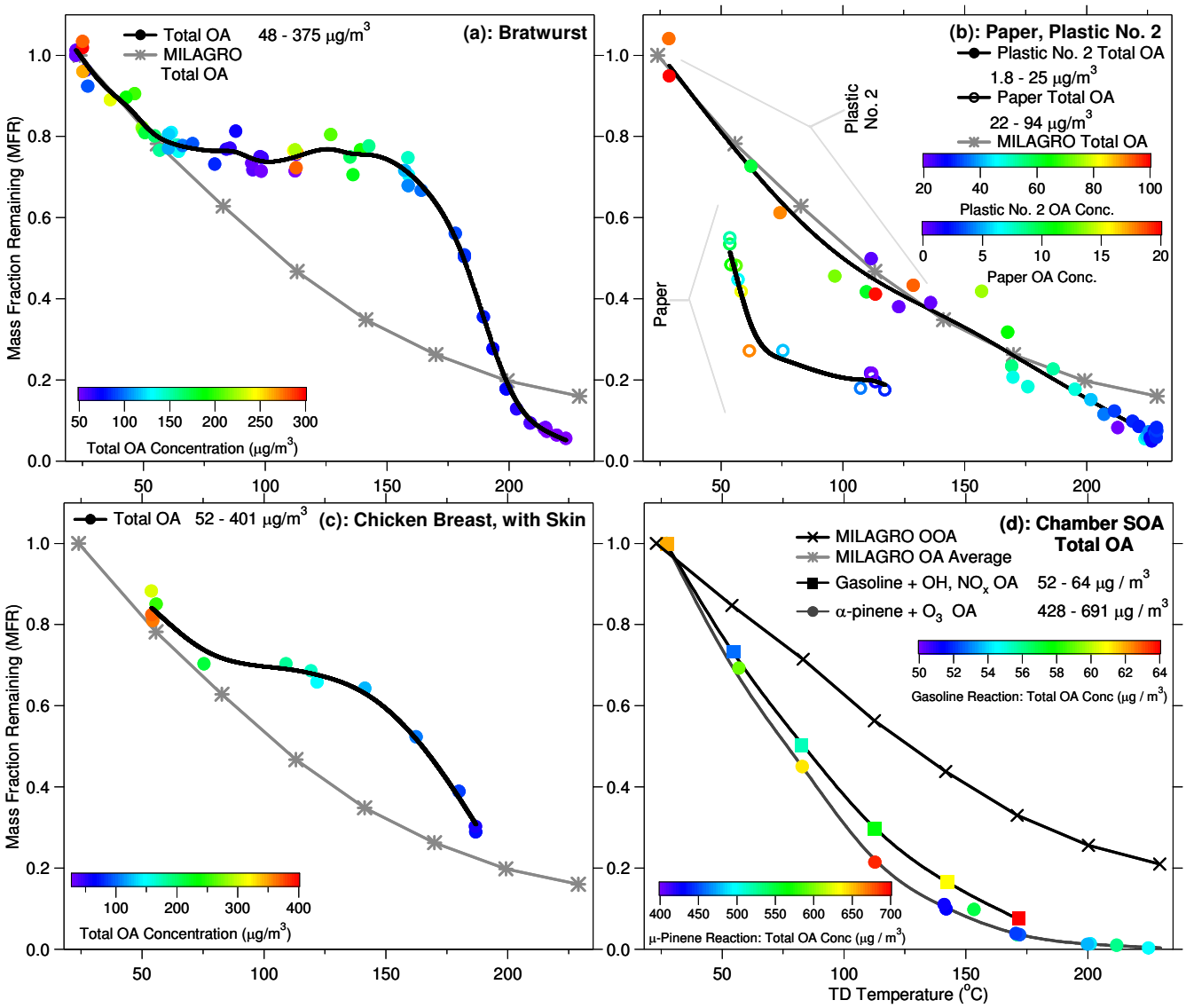
(a): Bratwurst
Total OA 48 - 375 µg/m3
MILAGRO Total OA
Total OA Concentration (µg/m3)
(b): Paper, Plastic No. 2
Plastic No. 2 Total OA 1.8 - 25 µg/m3
Paper Total OA 22 - 94 µg/m3
MILAGRO Total OA
Plastic No. 2 OA Conc.
Paper OA Conc.
Plastic No. 2
Paper
(c): Chicken Breast, with Skin
Total OA 52 - 401 µg/m3
Total OA Concentration (µg/m3)
(d): Chamber SOA Total OA
MILAGRO OOA
MILAGRO OA Average
Gasoline + OH, NOx OA 52 - 64 µg / m3
α-pinene + O3 OA 428 - 691 µg / m3
Gasoline Reaction: Total OA Conc (µg / m3)
µ-Pinene Reaction: Total OA Conc (µg / m3)
Mass Fraction Remaining (MFR)
TD Temperature (°C)

Figure S3